TU/e EINDHOVEN UNIVERSITY OF TECHNOLOGY

Online calibration of high-frequency partial discharge signals in three-phase belted power cables

Citation for published version (APA):
Wouters, P. A. A. F. (2005). Online calibration of high-frequency partial discharge signals in three-phase belted power cables. *IEE Proceedings - Science, Measurement and Technology*, *152*(2), 79-86. https://doi.org/10.1049/ip-smt:20051268

DOI:
10.1049/ip-smt:20051268

Document status and date:
Published: 01/01/2005

Document Version:
Publisher's PDF, also known as Version of Record (includes final page, issue and volume numbers)

Please check the document version of this publication:

• A submitted manuscript is the version of the article upon submission and before peer-review. There can be important differences between the submitted version and the official published version of record. People interested in the research are advised to contact the author for the final version of the publication, or visit the DOI to the publisher's website.
• The final author version and the galley proof are versions of the publication after peer review.
• The final published version features the final layout of the paper including the volume, issue and page numbers.

Link to publication

General rights
Copyright and moral rights for the publications made accessible in the public portal are retained by the authors and/or other copyright owners and it is a condition of accessing publications that users recognise and abide by the legal requirements associated with these rights.

• Users may download and print one copy of any publication from the public portal for the purpose of private study or research.
• You may not further distribute the material or use it for any profit-making activity or commercial gain
• You may freely distribute the URL identifying the publication in the public portal.

If the publication is distributed under the terms of Article 25fa of the Dutch Copyright Act, indicated by the "Taverne" license above, please follow below link for the End User Agreement:

www.tue.nl/taverne

Take down policy
If you believe that this document breaches copyright please contact us at:

openaccess@tue.nl

providing details and we will investigate your claim.

Download date: 04. Oct. 2023

Online calibration of high-frequency partial discharge signals in three-phase belted power cables

P.A.A.F. Wouters

Abstract: Partial discharge (PD) magnitudes from classical detection techniques are expressed in terms of apparent charges. Signals from HF/VHF/UHF techniques on substation components are often hard to express in this quantity because of complex signal excitation and propagation channels. A method to calibrate PD signals obtained during online inductive detection in medium voltage belted cables is described. Online inductive detection implies that the impedances of components present in substations essentially determine the detected PD signal magnitude. The use of belted cables means, that the coupling of a PD event to the conductors not only depends on the PD site within the cross-section of the cable or cable accessory, but also becomes dependent on the momentary phase angle. In addition, during signal propagation the signal magnitude may alter according to the propagation modes of a multi-conductor cable. These aspects are studied quantitatively by the use of theoretical modelling in addition to offline and online experiments. PD diagnostic equipment including pulse injection capability allows online calibration with sufficient accuracy, irrespective of the actual substation arrangement.

1 Introduction

At present various commercial partial discharge (PD) detection and location techniques are available for medium voltage (MV) cables [1–4]. These techniques are similar in the sense that they detect PDs within a bandwidth of several MHz, and location is realised through time domain reflectometry (TDR). The results are usually mapped as plots of PD activity against PD location. The techniques differ mainly in the way of energising the cable. For interpretation of the mappings, aspects like PD magnitude and intensity, total charge involved, distribution with phase angle, type and history of located fault (e.g. in cable joint or termination) are taken into account. This information is very useful, but only provides a snapshot of the cable state, valid under the specific circumstances during the test. To determine the cable condition, logging trends in PD activity is vital [5]. Trends during normal operation including load and temperature changes, but also during temporal over-voltages, can only be obtained by means of online techniques. Further, disconnecting the substation during installation can be omitted and no external power supply is required. These operational advantages make online techniques interesting from an economic perspective also.

The reason that online detection and location techniques are still at the development stage is their increased complexity as illustrated in Fig. 1.

Safely installing PD sensors, also during operation, implies inductive coupling. Offline systems usually extract their signals by means of capacitive coupling, requiring galvanic contact with (one of) the phase conductors. Inductive detection of the PD current can be achieved from suitable grounded conductors, without any safety hazard during installation and operation. Accessible coupling sites within a substation have to be identified [6].

Noise levels will be appreciably higher, since the cable under test is not isolated from the grid. In order to detect relatively low PD levels, say hundreds pC for paper-insulated-lead-covered (PILC) cables, advanced signal processing is required [7].

In contrast to offline techniques the far end of the cable is not open and clear PD signal reflection, required for TDR, is not guaranteed. The solution adapted here is two-sided measurement, which has been already successfully applied for long and/or branched cable connections [8]. An alternative solution is a transponder, a device that amplifies and sends back the signal at the far end after a well-defined time delay [9]. However, in case of a low S/N ratio the transponder responds also on noise signals, making this solution unfeasible in a noisy environment.

Two-sided measurements need some way of communication between the cable ends. Further, the time-bases of the equipment at both ends must be very accurately aligned in order to realise sufficient location accuracy. For communication a telephone connection (if present) and, for synchronisation, methods based on GPS [8] can be used. Alternatively, the cable under test can serve as a connection for both purposes. It forms a possible communication channel [10], and injected pulses at the near cable end may serve as reference time stamps at the far end [11].

In belted cables the phase conductors have a common screen resulting in an elliptical electric field [12]. The field eccentricity, defined as the ratio between the minimum and maximum electric field strength $\eta = E_{min}/E_{max}$, is shown in Fig. 2. The signal coupling to the conductors depends not only on the PD site within the cable dielectrics but now also on the momentary phase angle. Moreover, signal propagation results in rearranging the signal amplitudes over the

© IEE, 2005

IEE Proceedings online no. 20051268

doi:10.1049/ip-smt:20051268

Paper first received 24th February 2004

The author is with the Faculty of Electrical Engineering, Electrical Power Systems group, Eindhoven University of Technology, P.O. Box 513, 5600 MB Eindhoven, The Netherlands

E-mail: p.a.a.f.wouters@tue.nl

Authorized licensed use limited to: Eindhoven University of Technology. Downloaded on October 26, 2009 at 08:43 from IEEE Xplore. Restrictions apply.

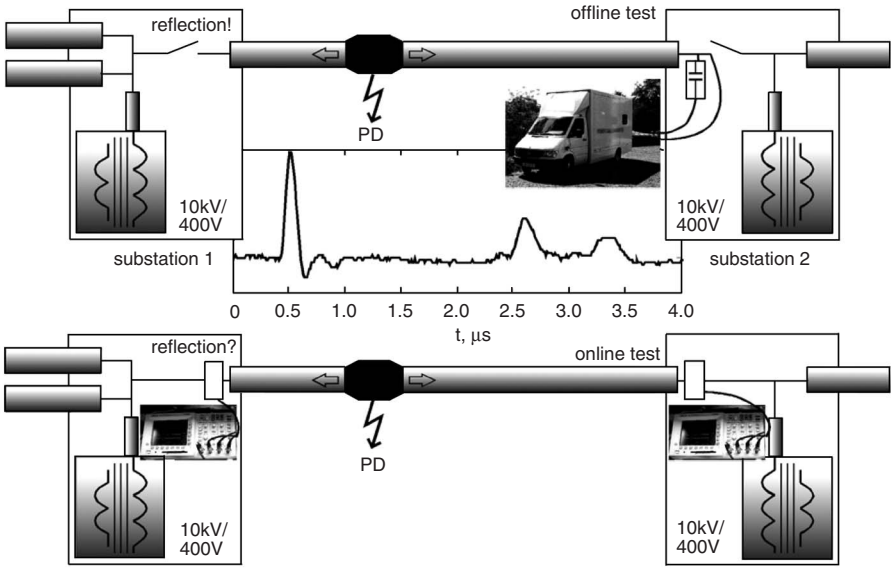

Fig. 1 *Typical test configuration during offline and online PD diagnostics*
Offline: The cable is disconnected from the grid and the cable is energised externally. The PD pulses can be located by TDR, because of full signal reflection at the far end (see inserted waveform)
Online: Signal reflection at the far end depends on the substation configuration, and TDR may be prohibited. Location is realised through double-sided detection

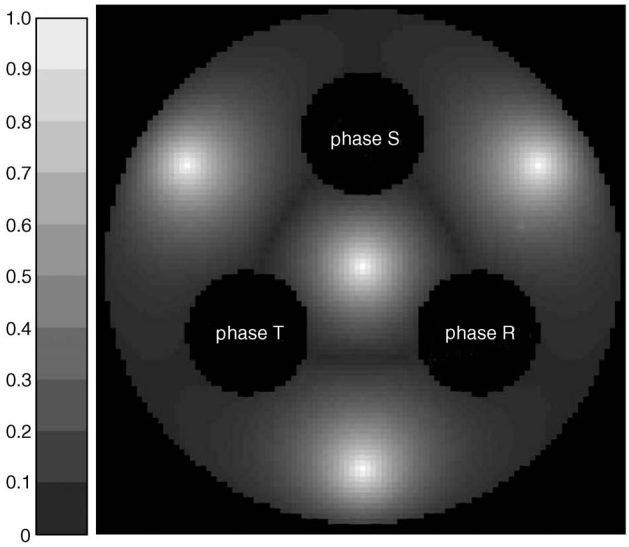

Fig. 2 *Eccentricity of electric field in artificial cable joint configuration*

conductors according to the cable propagation modes. Measured signals therefore not only reflect the PD occurrence itself, but also the signal excitation and propagation of the detection channel [13].

The present paper analyses aspects related to online calibration of PD signals obtained by inductive detection from belted MV cables. With respect to the PD magnitude, two major steps must be distinguished. First, in a multi-phase system a PD induces different charges in the conductors depending on its position and direction. Since this direction correlates with the electric field direction, the coupling strength to a specific conductor depends on the momentary phase angle for a rotating field vector. Signal detection from all phases would in principle allow interpretation of the measured amplitudes in terms of apparent charges, similar to offline tests. However, increased complexity resulting from multiple detection channels may hamper widespread introduction of an online diagnostic technique, and a compromise has to be found between complexity and performance. In Section 2 this aspect is analysed based on theoretical modelling of PD signal excitation and propagation in a three-phase belted cable. Second, the impedances of components present in substations determine the detected PD current magnitude. If all relevant impedances would be known beforehand, this information could be programmed into the detection equipment. However, these impedances depend on the specific configuration of the substation involved, depend also on details of the connections and ground loops, and may change according to new switch settings e.g. after maintenance. In Section 3 the option to include a pulse injection capability to detect the 'substation impedance' online is discussed. A pulse injection system was already considered for synchronisation purposes.

2 Signal excitation and propagation

Between the occurrence of a PD and signal detection at the end of a power cable three stages can be distinguished:
(i) The displaced charge in the cable dielectrics due to the PD induces charges in all cable conductors. If only one phase is energised, as in offline tests, the PD is directed according to the external field and will induce equal, but opposite charges in energised and grounded conductors. For a rotating field, as in online measurements, PDs can occur in various directions. The induced charge in a specific conductor depends on this direction, and may even be absent resulting in undetected events.
(ii) Next, the PD signal travels along the cable. In a symmetrical three-phase belted cable two distinct propagation modes exist. The shield-to-phase (SP) mode is the sum signal of all conductor currents with respect to the ground conductor. The phase-to-phase (PP) modes correspond to the difference signal from two-phase conductors. These modes have different propagation characteristics.
(iii) The signal is extracted at the cable end. If the signal is measured inductively from a ground connection, only the

Authorized licensed use limited to: Eindhoven University of Technology. Downloaded on October 26, 2009 at 08:43 from IEEE Xplore. Restrictions apply.

SP channel is detected. Signals obtained from a single phase conductor contain information on both SP and PP channels. This observation shows the importance of the choice of the sensor position in relation to the information to be obtained. Ideally, all channels are measured simultaneously, but from a practical point of view only a single sensor location may be chosen.

This Section discusses the excitation and propagation mechanism using an idealised defect; a spherical void within the dielectrics. In a linear field the PDs tend to concentrate at a phase angle between zero field and maximum field [14, 15]. Sufficient assumption for this pattern to occur is the presence of an internal field from charges resulting from previous PDs, which, together with the applied external field, makes up the total electric field inside the void. The field vector for a circular field is constant in amplitude and only changes direction. In this situation, no directional preference can exist, and consequently there is no relationship between PD occurrence and phase angle of the applied voltage. Simulations [12, 13] indicate that actually there can exist transitions of the PD pattern as a function of field eccentricity. Here, only the situations of (close to) a linear and circular field are considered.

2.1 Induced charge

For simplicity, it is assumed that the charge displacement from a PD neutralises the electrical field inside the void. For a spherical void in a surrounding medium with dielectric permittivity ε this corresponds to a surface charge density given by [12, 13]:

$$\sigma(\vartheta) = 3\varepsilon E_0 \cos(\vartheta - \vartheta_0) \tag{1}$$

The angle ϑ is taken with respect to the direction ϑ_0 of the applied field E_0, which is approximately homogeneous in the vicinity of the void. Because of the large difference between the time scale of the actual PD (ns) and the time scale associated with the bandwidth applied for PD detection in MV cables (MHz), a PD can be considered as a sudden emergence of a dipole field somewhere within the dielectrics. The field far from the charge distribution can be approximated by the field from a dipole $\boldsymbol{p}$ with equivalent charge Q (and $-Q$), corresponding to the amount of charge on one half sphere with radius a around $\vartheta = \vartheta_0$. The charges, placed in the centres of gravity of the semi-spheres, are separated over distance d:

$$\boldsymbol{p} = Q\boldsymbol{d} \quad \text{with} \quad Q = 3\pi\varepsilon a^2 E_0 \quad \text{and} \quad d = \tfrac{4}{3}a \tag{2}$$

The induced charge in the surrounding conductors can be calculated according to Ramo Shockley theory, see e.g. [16]. Figure 3 shows two hypothetical situations: (*a*) all conductors are grounded and a localised charge Q is present in the dielectrics; (*b*) earth screen and two phase conductors are grounded, one phase has potential U_A, and the charge Q is removed. The scalar potential functions U_1 (situation a) and U_2 (situation b) are related by Greens theorem:

$$\int\int\int_V (U_1 \Delta U_2 - U_2 \Delta U_1)\, dV = \int\int_S (U_1 \nabla U_2 - U_2 \nabla U_1) \cdot \boldsymbol{dS} \tag{3}$$

The surface S (indicated with broken lines in Fig. 3) enclosing volume V excludes all regions with conductors and charges, and can be subdivided in areas S_i around conductors i, and an infinitesimally small spherical area S_Q around the charge. The left hand side of (3) is zero because in the volume enclosed by S the Laplace equation is satisfied. In the first term of the right hand side the integrals over S_i vanish, because the potential U_1 is zero on all surfaces S_i; the integral over S_Q vanishes as well, because no charge is contained by S_Q for situation b (and U_1 is constant on S_Q). The integrals over the grounded surfaces in the second right hand side term do not contribute ($U_2 = 0$ on S_i with $i \neq A$). The remaining terms result in:

$$\int\int_{S_Q} U_2 \nabla U_1 \cdot \boldsymbol{dS} + \int\int_{S_A} U_2 \nabla U_1 \cdot \boldsymbol{dS} = 0$$

$$\Rightarrow \frac{Q_{ind}}{Q} = -\frac{U_2(\boldsymbol{r}_Q)}{U_A} \tag{4}$$

The last step follows from Gauss law, realising that U_2 is equal to U_A on S_A, and U_2 is constant on S_Q. The induced charge Q_{ind} in a conductor upon charge Q at position $\boldsymbol{r}_Q$ can be determined by applying a voltage U_A (e.g. 1 V) to this conductor and calculating the potential $U_2(\boldsymbol{r}_Q)$ at the location of the charge (e.g. numerically using electrostatic boundary or finite element method software). The apparent charge Q_{app} arising from the dipole according to (2) is found by calculating the charges induced by both $+Q$ and $-Q$ separated over distance d:

$$\frac{Q_{app}}{Q} = -\frac{U_2(\boldsymbol{r}_{+Q}) - U_2(\boldsymbol{r}_{-Q})}{U_A} \equiv -\frac{\boldsymbol{E}_{RS} \cdot \boldsymbol{d}}{U_A} \tag{5}$$

The apparent charge upon a PD can now directly be calculated from the electric field $\boldsymbol{E}_{RS}$.

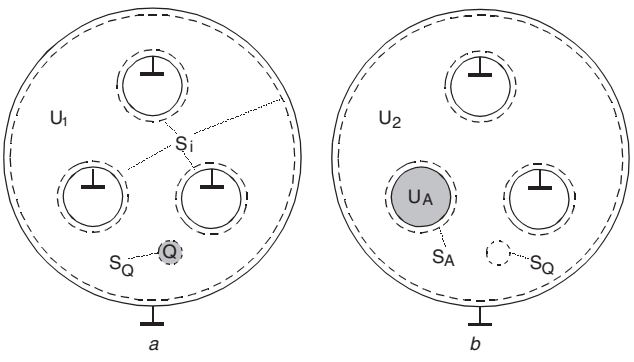

Fig. 3 *Hypothetical configurations to determine induced charges in cable (joint) conductors*

2.2 PD distributions

The Ramo Shockley considerations described above are applied to simulate PD patterns for a spherical void at different positions indicated with a, b, c in Fig. 4. Assumptions made for the modelling are (i) the void becomes fully neutralised upon a PD, (ii) the charge redistribution remains until the next PD, and (iii) the statistical time lag is small (e.g. 1% of one 50 Hz cycle) [13]. The simulations in Fig. 4 show $\varphi - q$ distributions (number of PDs per degree and per 1000 s against phase angle and apparent charge magnitude) for the three situations differing in field eccentricity: field mainly vertical aligned ($\eta = 0.2$, position a), circular field ($\eta = 1$, position b), and mainly horizontal aligned field ($\eta = 0.2$, position c). The phase angle is referred to the voltage applied to phase S; maximum voltage is reached at $\varphi = 0$. The patterns, which

Authorized licensed use limited to: Eindhoven University of Technology. Downloaded on October 26, 2009 at 08:43 from IEEE Xplore. Restrictions apply.

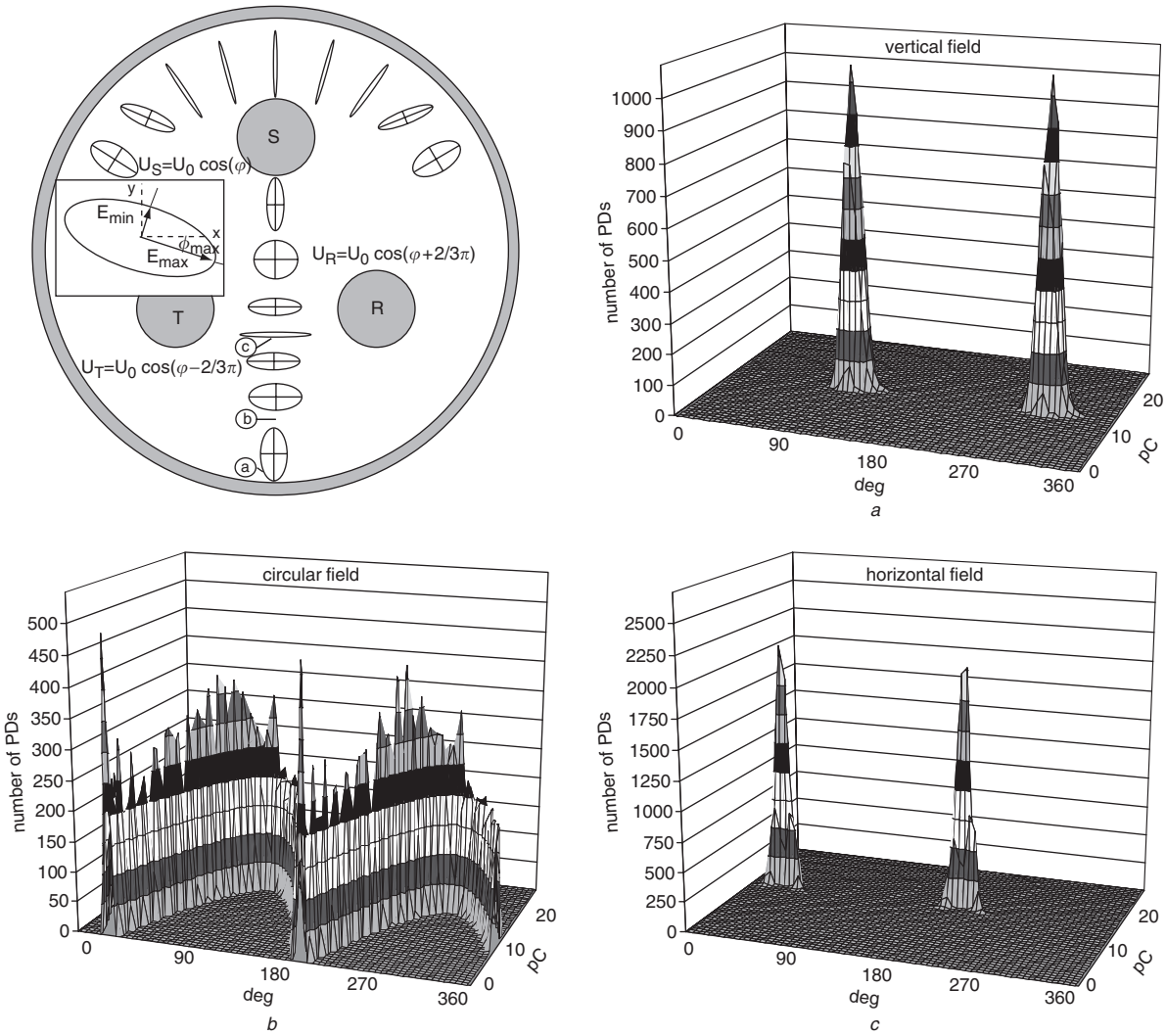

Fig. 4 *PD patterns from various locations within the dielectrics indicated with a,b,c differing in field eccentricity (see insert in top left figure)*

are obtained from the PD current at the earth screen, depend on the void position:

a) Vertical field: standard distribution occurring for (close to) linear fields with PD concentration between zero field and maximum field.

b) Circular field: despite the random PD occurrence, a sinusoidal pattern is observed owing to the PD direction dependent coupling to the earth screen.

c) Horizontal field: standard pattern for linear fields but 90° shifted, because maximum external field occurs a quarter of a cycle before/after maximum voltage at phase S.

This simplified engineering model for PDs in a spherical void already predicts the importance of the field eccentricity on the patterns. Observed patterns depend not only on the type of defect, but also on the phase angle dependent coupling to the conductor from which the signal is extracted. Although this complicates interpretation when compared to offline tests with linear fields, it may prove to give additional information on the defect.

2.3 PD signal propagation

The distinct propagation channels can modify the PD signal amplitudes. Therefore, patterns can to some extent depend on the cable length between defect and substation. The signal propagation modes for the PD currents in frequency domain for a symmetrical three-phase belted cable are given by [12, 17]:

$$(I_R+I_S+I_T)(z)=(I_R+I_S+I_T)(0)\mathrm{e}^{-\gamma_{SP}(\omega)z}$$

$$\begin{pmatrix} I_R-I_S \\ I_S-I_T \\ I_T-I_R \end{pmatrix}(z)=\begin{pmatrix} I_R-I_S \\ I_S-I_T \\ I_T-I_R \end{pmatrix}(0)\mathrm{e}^{-\gamma_{PP}(\omega)z} \quad (6)$$

The propagation coefficient $\gamma(\omega)$ is different for distinct modes. If the signal is extracted from one phase, e.g. phase R, the following combination of modes is measured:

$$\begin{aligned} I_R(z)=&\tfrac{1}{3}(I_R+I_S+I_T)(0)e^{-\gamma_{SP}(\omega)z} \\ &+\tfrac{1}{3}(I_R-I_S)(0)e^{-\gamma_{PP}(\omega)z} \\ &-\tfrac{1}{3}(I_T-I_R)(0)e^{-\gamma_{PP}(\omega)z} \end{aligned} \quad (7)$$

If the attenuation in both channels differs considerably then, after a long propagation distance, either the first term or the last two terms will dominate the signal at the detection side. Figure 5 shows two simulations of the PD magnitude against phase angle for these extreme situations for the case of a circular field. The number of PDs is indicated with grey scaling (in fact, this representation is a top view of plots similar to Fig. 4). Depending on the

Authorized licensed use limited to: Eindhoven University of Technology. Downloaded on October 26, 2009 at 08:43 from IEEE Xplore. Restrictions apply.

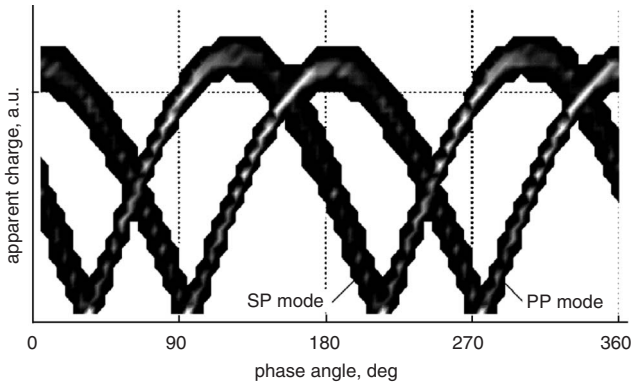

Fig. 5 *Top view of PD pattern obtained from phase R against phase angle and PD magnitude for circular field with either SP-channel or PP-channel dominant*

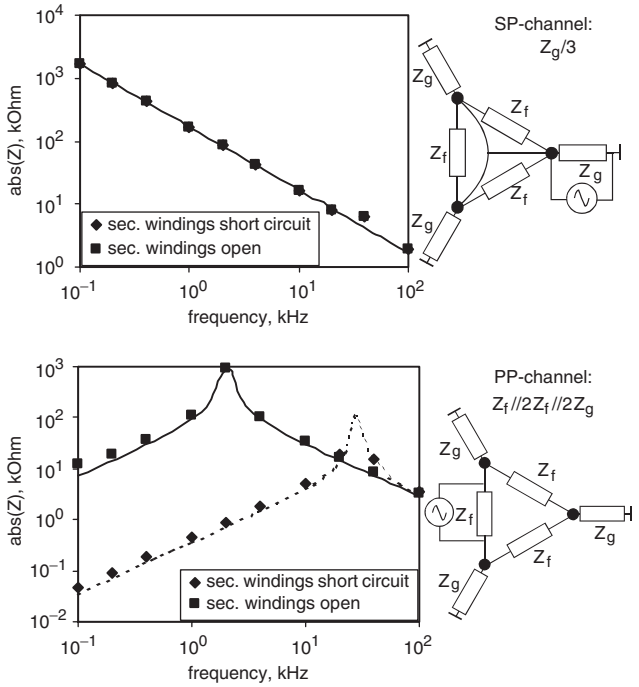

Fig. 6 *Transformer impedance between 100 Hz and 100 kHz with open (solid line) and short-circuited (broken line) low-voltage side*
SP-channel: impedance between three interconnected phases and ground
PP-channel: impedance between two phases with third phase floating

detected mode, either SP or PP, the pattern is shifted over about 60°. For shorter cables both modes coexist in a ratio, which depends on the cable length. Note, that the pattern for the SP mode is similar to Fig. 4*b*, since there the signal is obtained from the screen, which only contains the SP mode.

3 Substation impedance

A PD pulse arriving at the cable end will be partly reflected and be partly transmitted depending on the impedances of components present in the substation, such as a distribution transformer and leaving cables. Cables can be considered as real (characteristic) impedances; the transformer impedance will be frequency dependent. Also the (ground) connections may contribute to the impedance, owing to the self-inductance of possibly large loops. For a three-phase system transmission and reflection can be described in terms of matrices [18]. In the following, however, mainly the SP channel is considered. Further, we assume that the loads from the substation to a large extent have three-fold symmetry like the cable. In this approximation the relevant transmission and reflection coefficients are scalar quantities. Also transmission line effects, which may have some effect in large substations, are disregarded.

3.1 Modelling substation impedances

In a study aiming for the feasibility of using the medium voltage grid for power line communication, the behaviour of a distribution transformer was investigated [10]. The impedance of a distribution transformer (400 kVA–10 kV/380 V) was measured up to a frequency of 100 kHz (CENELEC A-band). The results for two situations are shown in Fig. 6:

SP-impedance: all phases are interconnected, and the impedance between phases and ground is measured.

PP-impedance: the impedance between two phases is determined with the third phase floating.

The transformer is modelled with lumped impedances: Z_f between the phases, and Z_g between phase and ground (see inserts, Fig. 6). Impedance Z_f consists of a coil inductance L_f parallel to a capacitance C_f, which takes into account the capacitive coupling between the windings; Z_g corresponds to the capacitance C_g between coil and transformer core/housing. The curves in Fig. 6 are fits to the measured symbols using $C_g = 315$ pF, $C_f = 260$ pF, and $L_f = 17$ H or 0.086 H depending on the load at the low voltage side (open or short circuit). For frequencies above about 50 kHz the absolute impedance exhibits $1/f$ behaviour under all tested conditions. Apparently, capacitive coupling becomes dominant. This result suggests that the transformer can be modelled as a lumped capacitance. If the SP-channel is considered, the impedance consists of three phases in parallel with ground as the return current path. It is therefore expected that a distribution transformer typically behaves like a capacitor with a value close to 1 nF. For large transformers, e.g. connecting the MV grid to transmission lines, this capacitance can be higher.

3.2 Signal propagation along PILC cable

A 4 km three-phase belted PILC cable was loaded (offline) on both sides with several impedances, resistive as well as capacitive. Load impedances of 10 Ω and 100 Ω covering the range of actual cable characteristic impedances, 1 nF and 10 nF representing transformers (including extra capacitance from connecting cables) were chosen as being indicative for the performance of the propagation channel. This impedance is particularly important in case of inductive signal coupling as anticipated for the online system. The transfer functions shown in Fig. 7 relate the applied current I_0 exciting the injection coil to the resulting current I_{out} in the detection circuit. Signal coupling was accomplished by means of air coils (Rogowski) with a mutual inductance of 1.86 μH. The transfer function for a cable with length ℓ and characteristic impedance Z_0 is given by [10]:

$$H(\omega) = \frac{I_{out}}{I_0} = \tfrac{1}{2}\mathrm{j}\frac{\omega M_1}{Z_0} \cdot \frac{\tau_1(\omega) \cdot \tau_2(\omega)\mathrm{e}^{-\gamma(\omega)\ell}}{1 - \rho_1(\omega)\rho_2(\omega)\mathrm{e}^{-2\gamma(\omega)\ell}} \qquad (8)$$

Authorized licensed use limited to: Eindhoven University of Technology. Downloaded on October 26, 2009 at 08:43 from IEEE Xplore. Restrictions apply.

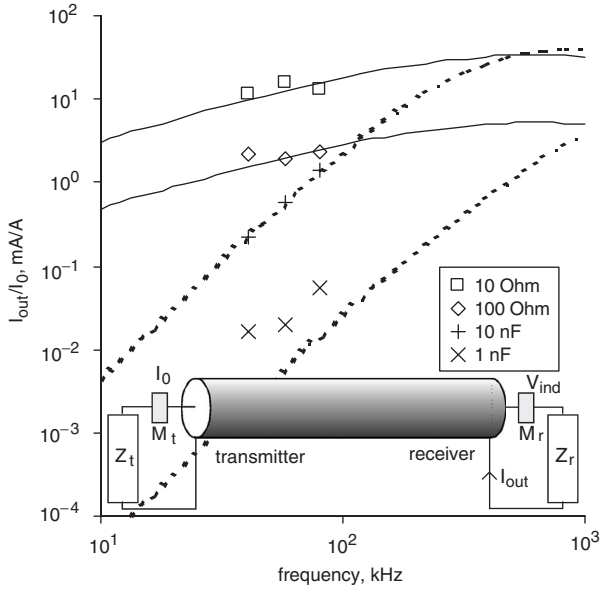

Fig. 7 *Extrapolation up to 1 MHz of transfer functions (lines) based on experimentally determined values (symbols) within the CENELEC A-band*

with τ and ρ the current transmission and reflection coefficients at the cable to substation transitions at both cable ends (index 1,2), and M_1 the mutual inductance at the injection side. The denominator in the right hand factor of (8) is approximately 1 because of signal attenuation over 4 km, resulting in:

$$|H(\omega)| = \frac{\omega M_1}{2Z_0}|\tau_1(\omega)||\tau_2(\omega)|e^{-\alpha(\omega)\ell}$$
$$\text{with} \quad \tau_{1,2} = \frac{2Z_0}{Z_0 + Z_{1,2}} \tag{9}$$

The calculated curves are based on two fit parameters obtained from the measured values, indicated with symbols: cable impedance $Z_0 = 40, \Omega$, and damping factor owing to skin effect $\alpha(\omega) = 2.5 \times 10^{-7}\sqrt{\omega}\,\mathrm{m}^{-1}$ (ω in s^{-1}) [10]. The large range in values for the transfer function proves the high sensitivity of the system performance with substation impedance. It should be noted, that a transformer will not behave as a perfect capacitor up to frequencies relevant for PD detection (several MHz), but may exhibit some resonances. One obvious resonance occurs due its capacitance together with the self-inductance of the connections, which is in the order of several hundred nH. These resonances, which depend on the precise installation details of the equipment, show that *a priori* prediction of the substation impedances from known individual component values is quite awkward. Therefore, it is aimed to include a calibration method within the online equipment.

3.3 Online acquisition of the substation impedance

Pulse injection, required for time base alignment in case of double-sided measurement, can also be of use for determining relevant substation impedances [19] online. A coil, placed around a conductor in the substation, is basically a weakly-coupled transformer consisting of the primary injection coil and the secondary circuit formed by the substation connections. Weakly means that primary and secondary circuits can be described independently: the primary excitation current results in a known induced voltage over the impedances present in the secondary substation circuit.

A well-defined pulse, with its energy concentrated mainly in the low MHz range, can be realised by discharging a capacitor over the self-induction of the injection coil [19]. The resulting oscillation can be blocked to obtain a sinusoidal waveform with a duration of e.g. a half cycle. For injection, a Rogowski coil with a mutual inductance of $M = 42$ nH was mounted around the earth screen (placed beyond the last ground connection [6]) of an incoming cable.

From the measured secondary waveforms I_{sec} at the injection side, and the known injection current I_{inj}, the values of the relevant lumped impedances can be deduced:

$$I_{\mathrm{sec}} = \frac{j\omega M}{Z_{inj} + (\sum 1/Z_i)^{-1}} I_{inj} \tag{10}$$

Z_{inj} represents the impedance of the cable containing the injection coil; the sum in the denominator includes all impedances closing the current path. Figure 8 illustrates a cable connection where pulses are injected in either the left or right cable end. In both cases the secondary current is measured over the same cable screen as injection takes place by means of commercially available current probes (1 V/A). The characteristic impedances of two leaving cables, and the distribution transformer close the injection current path in the right substation. The latter impedance, however, hardly contributes here. In contrast, for injection in the left substation only the transformer with its connection closes the current path. The fits were obtained by using characteristic impedances of 12 Ω (SP channel), and a total value of 3 nF for the transformer (1 nF) together with its connection (2 nF) as dominant impedances. Besides the circuit self-inductance, additional circuit resistance to take into account skin effect and radiation losses was introduced in order to get good agreement. In principle, using the acquired values of the substation impedances, the cable propagation characteristics can be also determined when the signal at the far end is measured as well.

4 Discussion

The ultimate purpose of PD calibration is to express the detected signal magnitudes in a quantity, which is independent of the measuring system. In classical PD testing apparent charge is used, which indicates the amount of charge induced in external electrodes accessible for PD detection. Calibration is realised by injecting a known charge over the electrodes. For PD techniques involving signal propagation this calibration method cannot be applied, basically because the propagation channel from PD site to terminals is crucial for the content of the measured signals at the terminals of the device. For instance, acoustic and electric (VHF/UHF) PD detection in generators do not scale directly because of their different propagation paths [20], making absolute calibration awkward.

Cables are easier to model, because of their relatively simple geometry. Knowing the cable propagation characteristics, the substation component impedances and the sensor bandwidth, the detected signals can be traced back to the original induced charges at the defect. The accuracy by which these charges can be established depends, amongst others, on the uncertainty in the overall substation impedance, which is in the order of 10–20% if the pulse injection method is applied. For PD magnitudes this is sufficient, since often the uncertainty is much higher for other reasons, e.g. not accurately known cable properties.

Authorized licensed use limited to: Eindhoven University of Technology. Downloaded on October 26, 2009 at 08:43 from IEEE Xplore. Restrictions apply.

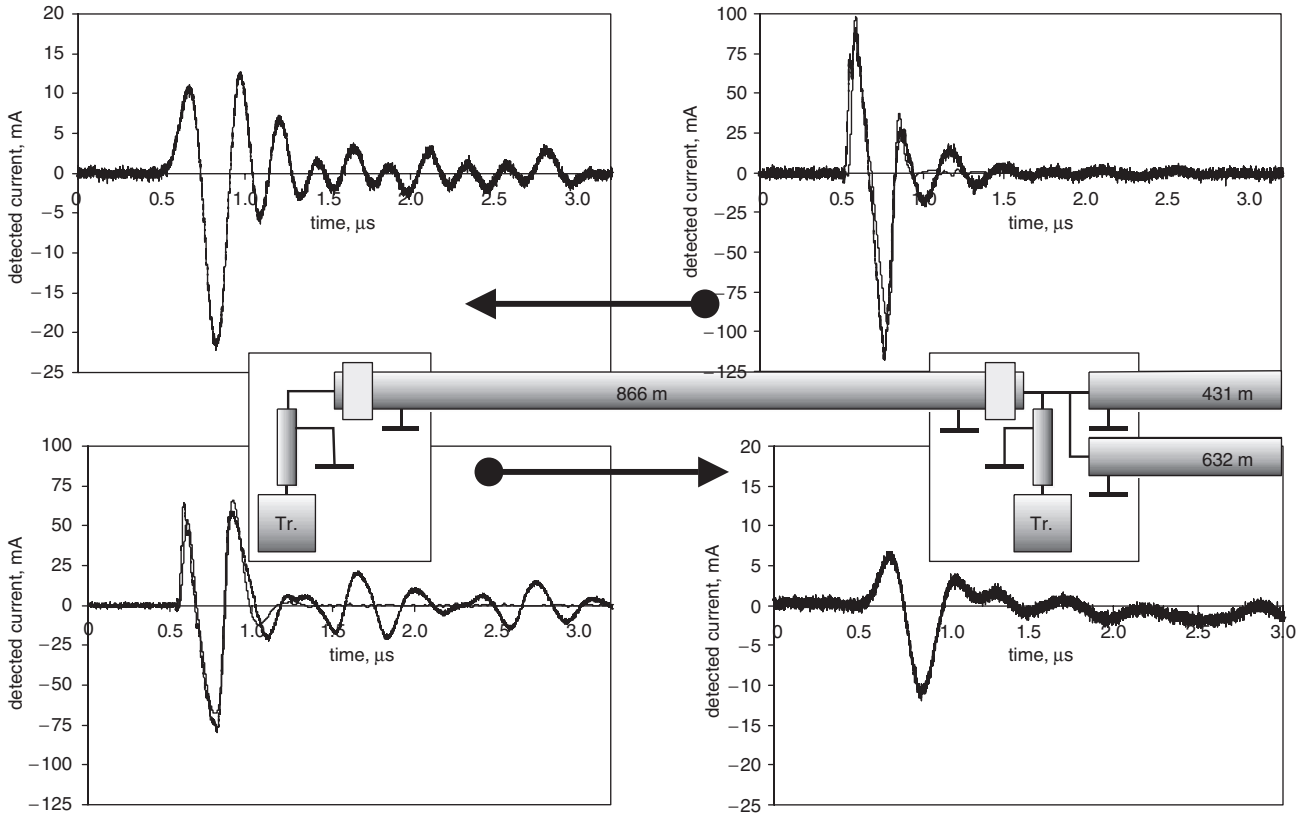

Fig. 8 *Response on injection pulses, measured at two substations connected by PILC cable, including calculated waveform (thin line) at injection side*
Top figures: injection cable end loaded with distribution transformer (Tr.) and two leaving cables
Bottom figures: injection cable end only loaded with distribution transformer

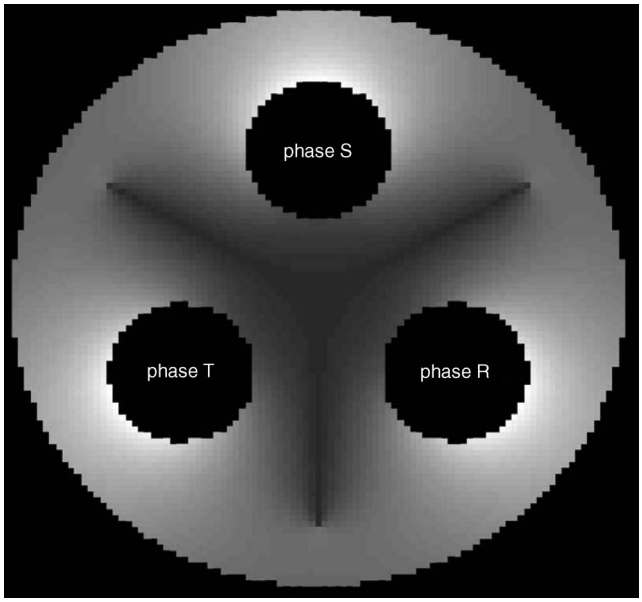

Fig. 9 *Calibration factor between apparent charge in earth screen and real charge indicating high (light areas) and low (dark areas) sensitivity for PD detection*

In comparison, VHF/UHF techniques in generators and transformers usually fail to have adequate calibration methods for life components. The merits of those techniques can be attributed to the fact that they concern online diagnostics, which allows detection of trends in PD behaviour.

For belted cables an additional parameter is introduced, related to the elliptical nature of the electric field. Especially, when the PDs are extracted from only one conductor, e.g. the cable earth screen, the complete information on the original PD is not obtained. This can possibly result in undetected PD events. Figure 9 indicates the theoretical calibration factor between apparent and real charge for PDs in case they occur in the direction of maximum applied field. The dark region in the centre corresponds to relatively low sensitivity. It should be noted, however, that real defects in PILC cables are much larger in size than the simulated void, and also PDs will not occur only in the direction of the external (maximum) field. Therefore, some signal coupling to the earth screen will still take place.

5 Conclusion

For online PD detection and location in MV cables inductive signal coupling is preferred from an installation and a safety point of view. The technical complications involve, among others, the calibration of the PD magnitude, since impedances of components present in the substations load both ends of the cable under test. Applying pulse injection as a means of online determination of substation impedances is promising and will be investigated further in order to extract cable propagation characteristics as well.

Belted cables have multiple PD excitation and propagation channels. If only one channel is detected, e.g. from inductive coupling to the earth screen, information may be lost for PDs occurring at certain phase angles in some parts of the cable (or accessory) cross-section. However, the PD amplitudes and distributions are still unambiguous for a

Authorized licensed use limited to: Eindhoven University of Technology. Downloaded on October 26, 2009 at 08:43 from IEEE Xplore. Restrictions apply.

given sensor position in the sense that results from different techniques can be translated to the same values for the apparent charge magnitude. Whether detection of all channels is required will be basically a compromise between costs and complexity, and technical performance. This issue can be resolved only after obtaining sufficient practical experience with online detection. In any case, the ability to detect PDs from power cables in service promises to be a major step forward, since it will allow monitoring of trends in PD behaviour over a long time.

6 Acknowledgments

This research is supported by the following Dutch parties: Technology Foundation STW, applied science division of NWO and the technology programme of the Ministry of Economic Affairs; Eindhoven University of Technology; KEMA Nederland; Continuon Netbeheer; ENECO Netbeheer. Additionally, Cor Verhoeven, Peter van Roij (ESSENT) for making available a 4 km PILC cable connection, and Peter van der Wielen, Paul Wagenaars, Hennie van der Zanden (TUE), for their contributions to the field tests, are gratefully acknowledged.

7 References

1 Steennis, E.F., Hetzel, E., and Verhoeven, C.W.J.: 'Diagnostic medium voltage cable test at 0.1 Hz'. Proceedings of the 3rd Int. Conf. on Insulated Power Cables, Versailles, France, June 1991, pp. 408–414
2 Lemke, E., and Schmiegel, P.: 'Complex discharge analysing (CDA) – an alternative procedure for diagnosis tests on HV power apparatus of extremely high capacity'. Proc. of 9th Int. Symp. on High Voltage Engineering, Graz, Austria, August 1995, Vol. 5, pp. 5617/1–5617/4
3 Gulski, E., Smit, J.J., Seitz, P.N., and Smit, J.C.: 'PD measurement on site using oscillating wave test system'. Proc. of IEEE Int. Symp. on Electrical Insulation, Arlington, USA, June 1998, Vol. 2, pp. 420–423
4 Mashikian, M.S.: 'Partial discharge location as a diagnostic tool for power cables'. IEEE Power Engineering Society Winter Meeting 2000, January 2000, Vol. 3, pp. 1604–1608
5 Orton, H.E.: 'Diagnostic testing of in-situ power cables – an overview'. Proc. of 13th Int. Symp. on High Voltage Engineering, Delft, The Netherlands, August 2003
6 van der Wielen, P.C.J.M., Veen, J., Wouters, P.A.A.F., and Steennis, E.F.: 'Sensors for online PD detection in MV power cables and their locations in substations'. Proc. of 7th Int. Conf. on Properties and Applications of Dielectric Materials, Nagoya, Japan, June 2003, Vol. 1, pp. 215–219
7 Veen, J., and van der Wielen, P.C.J.M.: 'The application of matched filters to PD detection and localization', *IEEE Electr. Insul. Mag.*, 2003, **19**, (5), pp. 20–26
8 Steennis, E.F., Ross, R., van Schaik, N., Boone, W., and van Aartrijk, D.M.: 'Partial discharge diagnostics of long and branched medium-voltage cables'. Proc. of IEEE 7th Int. Conf. on Solid Dielectrics, Eindhoven, The Netherlands, June 2001, pp. 27–30
9 Michel, M.: 'Moving towards a complete online condition monitoring solution'. Proc. of 17th Int. Conf. and Exhibition on Electricity Distribution, Barcelona, Spain, May 2003
10 Wouters, P.A.A.F., and van der Wielen, P.C.J.M.: 'Effect of cable load impedance on coupling schemes for MV power line communication'. Proc. of IEEE Bologna PowerTech Conf., Bologna, Italy, June 2003
11 van der Wielen, P.C.J.M., Wouters, P.A.A.F., Veen, J., and van Aartrijk, D.M.: 'Synchronization of online PD detection and localization setups using pulse injection'. Proc. of 7th Int. Conf. on Properties and Applications of Dielectric Materials, Nagoya, Japan, June 2003, Vol. 1, pp. 327–330
12 van der Wielen, P.C.J.M., Steennis, E.F., and Wouters, P.A.A.F.: 'Fundamental aspects of excitation and propagation of online partial discharge signals in three-phase medium voltage cable systems', *IEEE Trans. Dielect. Electr. Insul.*, 2003, **10**, (4), pp. 678–688
13 Wouters, P.A.A.F., and van der Wielen, P.C.J.M.: 'Implications of online PD measurement on phase distributions for three-phase belted MV cables'. Proc. of 7th Int. Conf. on Properties and Applications of Dielectric Materials, Nagoya, Japan, June 2003, Vol. 1, pp. 83–87
14 Kreuger, F.H.: 'Partial discharge detection in high-voltage equipment' (Butterworths, London, 1989)
15 Tanaka, T.: 'Partial discharge pulse distribution pattern analysis', *IEE Proc.-Sci. Meas. Technol.*, 1995, **142**, (1), pp. 46–50
16 Wetzer, J.M., and van der Laan, P.C.T.: 'Prebreakdown currents: basic interpretation and time-resolved measurements', *IEEE Trans. Electr. Insul.*, 1989, **24**, (2), pp. 297–308
17 Paul, C.R.: 'Decoupling the multiconductor transmission line equations', *IEEE Trans. Microw. Theory Tech.*, 1996, **44**, (8), pp. 1429–1440
18 Djordjević, A.R., and Sarkar, T.K.: 'Analyis of time response of lossy multiconductor transmission line networks', *IEEE Trans. Microw. Theory Tech.*, 1987, **35**, (10), pp. 898–907
19 Wouters, P.A.A.F., van der Wielen, P.C.J.M., and Steennis, E.F.: 'Challenges related to development of an online PD detection and localisation system'. Proc. of 18th Nordic Insulation Symp., Tampere, Finland, 2003, pp. 3–10
20 Brammer, R., Ullberg, B., Sandstedt, J., Bengtsson, T., Hedberg, J., Dahlberg, L-G., Sörqvist, T., and Andersson, I.: 'Acoustic PD testing of cable joints in a powerformer'. Proc. of 17th Nordic Insulation Symp., Stockholm, Sweden, June 2001, pp. 71–78

Authorized licensed use limited to: Eindhoven University of Technology. Downloaded on October 26, 2009 at 08:43 from IEEE Xplore. Restrictions apply.